PAPER

Selective release of a potent anticancer agent from a supramolecular hydrogel using green light†

Johannes Karcher,[a] Susanne Kirchner,[a] Anna-Lena Leistner,[a] Christian Hald,[a] Philipp Geng,[a] Tobias Bantle,[a] Peter Gödtel,[a] Juliana Pfeifer[b] and Zbigniew L. Pianowski ✶[ac]

Light-triggered drug release from hydrogels is a promising method to improve efficiency of antitumor treatment, as an alternative to existing photodynamic therapies. Here we report a photochromic supramolecular low-MW hydrogel that can quickly and selectively release a physically encapsulated potent anticancer agent upon green light irradiation under physiological conditions.

Numerous advanced drug delivery systems are based on hydrogels, which can protect labile drugs from premature degradation, or maintain constant drug concentration in blood over prolonged periods of time.[1] Macroscopic gels can be used in the form of implants, whereas microgels allow for oral and pulmonary delivery, and nanogels can be systemically administered into the bloodstream of patients.[2,3] While covalent hydrogels are based on polymers (gelatin, alginate, agarose), supramolecular low-MW hydrogels[4] can be formed by mutual non-covalent interactions of short linear oligopeptides,[5–10] nucleobases,[11] or urea derivatives.[12,13] Hydrogels can be triggered by external stimuli, such as pH changes or enzymes, to release encapsulated drugs in a controllable fashion.[14–17] Light is a particularly attractive stimulus in this context,[18] because it can be applied on living organisms with high spatiotemporal precision without their permanent contamination. Light-responsive supramolecular hydrogels,[19–23] often tailored to particular applications like cargo release,[24,25] or shape memory,[26] frequently contain molecular photoswitches – structures that can reversibly interconvert between two photo-isomers upon irradiation.[27] The associated modulation of geometry, polarity, or other molecular properties may elicit macroscopic effects in various materials.[28–33]

Common photoswitches are usually triggered with UV light, but this frequency does not penetrate living cells or tissues

efficiently. Therefore, photoswitches triggered with visible light are developed for applications in complex biological systems.[34–41] In azobenzenes, such a bathochromic shift is usually associated with loss of thermal stability. Notable exceptions are *ortho*-fluorinated azobenzene derivatives, mutually switchable with green (*trans* → *cis*) and violet (*cis* → *trans*) light between two photoisomers, which are thermally (meta)stable at ambient conditions.[42] This motif was used in numerous light-triggered materials[43–45] and biological applications.[46–50]

Our group has previously merged the excellent hydrogelation propensity of amphiphilic cyclic dipeptides[51–53] with the photoswitchable azobenzene motif. The resulting biocompatible photochromic hydrogels can reversibly dissipate to fluids upon irradiation (due to the reversible polarity change ensuing azobenzene photoisomerization) under physiological conditions, and concomitantly release encapsulated bioactive substances.[54,55] However, due to the non-covalent nature of the encapsulation, substantial spontaneous cargo diffusion ("leaking") from loaded gels in darkness was often observed, thus compromising selectivity of the light-triggered release. Moreover, hydrogels based on the bis-*ortho*-fluoroazobenzene photochrome (sensitive on green light) only formed above the critical gelator concentration (CGC) of 40 g L^{-1}. Consequently, complete gel dissipation required relatively long irradiation time (≥3 h).[55] The selectivity and timespan were sufficient for a proof-of-principle demonstration of green-light control over bacterial growth by photocontrolled antibiotic release. However, these parameters must be improved before therapeutic applications were conceivable for human subjects.

In this communication, we report a successful strategy towards decreasing the CGC, and increasing selectivity of the light-induced cargo release in photochromic supramolecular hydrogels based on cyclic dipeptide gelators.

It is known that aromatic C–F bonds may generate new non-covalent interactions in proximity of the fluorine atoms.[56] We hypothesized that the tetra-*ortho*-fluorinated azobenzene

[a]*Institut für Organische Chemie, Karlsruher Institut für Technologie, Campus Süd, Fritz-Haber-Weg 6, 76131 Karlsruhe, Germany. E-mail: pianowski@kit.edu*

[b]*Institut für Funktionelle Grenzflächen IFG, Karlsruher Institut für Technologie, Campus Nord, Hermann-von-Helmholtz Platz 1, 76344 Eggenstein-Leopoldshafen, Germany*

[c]*Institute of Biological and Chemical Systems – FMS, Karlsruher Institut für Technologie, Campus Nord, Hermann-von-Helmholtz Platz 1, 76344 Eggenstein-Leopoldshafen, Germany*

† Electronic supplementary information (ESI) available: Synthesis, spectroscopy, rheology, electron microscopy, photochromism and chromatography data. See DOI: 10.1039/d0ra08893e

(TFAB) should improve supramolecular association of the fibre subunits and thus decrease the critical gelator concentration in comparison to the previously demonstrated hydrogelator, based on the bis-*ortho*-fluorinated azobenzene.[55]

The hydrogelator **1** (Fig. 1) has been prepared according to the synthetic route depicted in Schemes 1 and S1.† The crucial intermediate – bis-fluorinated (*S*)-phenylalanine analogue **5** was synthesized from 4-bromo-2,6-difluoroaniline (**4**) and the protected (*R*)-iodoalanine (**3**) using Negishi coupling. Mills reaction of **5** with *in situ* generated 2,6-difluoronitrosobenzene (**6**) and subsequent methyl ester hydrolysis provided the photochromic amino acid derivative **8** (>96% ee, Fig. S14†), which upon coupling to an (*S*)-lysine derivative and cyclization of the linear dipeptide **11** yielded the hydrogelator **1**. Additionally, full deprotection of **8** may provide an enantioselective access to the amino acid **12**, previously used as racemate for biosynthetic incorporation into luciferase protein using the amber codon suppression method.[50]

Irradiation of **1** in aqueous solution (phosphate-buffered saline, pH 7.4 – a typical buffer for biological experiments, abbreviated below as **PBS**, composed of 8 g NaCl, 0.2 g KH$_2$PO$_4$, 1.15 g Na$_2$HPO$_4$, and 0.2 g KCl in 1 L of water) with green light (530 nm LED, 7 mW cm^{-2}) until equilibration resulted in the mixture containing 89% of the *cis*-**1**. Further exposure of this solution on violet light (410 nm LED, 9 mW cm^{-2}) produced a mixture containing 23% of the *cis*-**1** (Fig. S1 and Table S1†). In darkness, the thermal *cis* → *trans* isomerization of **1** at r.t. is practically suppressed. At 60 °C, the thermal isomerization of *cis*-**1** ($t_{1/2}$ = 70.9 ± 0.6 h at 60 ± 2 °C, in MeCN, Fig. S2† left) is slightly faster than for the unsubstituted *cis*-TFAB ("**F4**", $t_{1/2}$ = 92 h at the same temperature in MeCN[42]).

Another common limitation for *in vivo* applications of azobenzene derivatives in biological systems is their reduction with biogenic thiols to arylhydrazines. The compound **1** is resistant (below 8% of degradation within 6 days of incubation, Fig. S2† right) to 5.0 mM reduced glutathione solution – an established model of the intracellular redox environment.
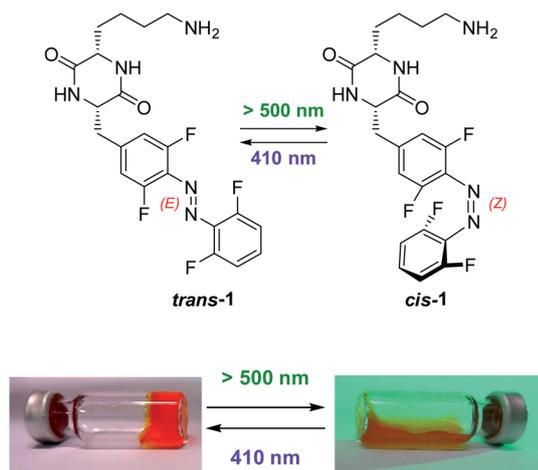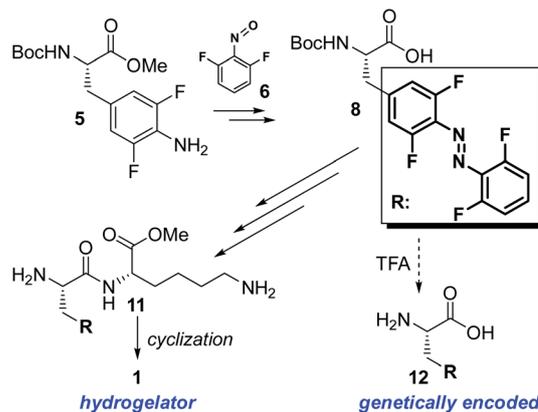

Fig. 1 Photochromic cyclic dipeptide *trans*-**1** is a low-MW supramolecular hydrogelator, while its photoisomer *cis*-**1** forms non-viscous fluids at the same concentrations; a photochromic hydrogel based on **1** (here, 17 g L^{-1} of **1** in PBS, pH 7.4) reversibly dissipates to a fluid upon irradiation with green light.

Scheme 1 Schematic depiction (detailed on the Scheme S1†) of synthesis of the photochromic supramolecular hydrogelator **1** bearing the "TFAB" photoswitch (framed and abbreviated as **R**). Upon deprotection, the molecule **8** can also yield the TFAB-substituted (*S*)-alanine **12**, which has previously been biosynthetically incorporated into proteins using the amber codon suppression technique.[50]

The compound **1** forms stable and homogenous hydrogels in aqueous solutions under physiological conditions (PBS buffer, pH 7.4, Fig. 1) at the concentrations ≥15 g L^{-1} of **1** (Table S2†). Although this value is still over a magnitude higher above the most efficient UV-light-triggered super(organo)gelators (CGC < 0.1 wt%),[21,22] our material enables drug release in water with visible light – not reported for supergelators yet.

After 30 minutes of irradiation with green light (530 nm, power input of 3 W, 7 mW cm^{-2}, 22 ± 2 °C), hydrogels containing 15 g L^{-1} or 17 g L^{-1} of **1** turned into homogenous fluids without any mechanical stimulation (Fig. 1 and S4†), while the hydrogel containing 20 g L^{-1} of **1** needed slight mechanical stimulation (*e.g.* by shaking the vial). Gels containing 30 g L^{-1} of **1** or above withstood 60 min of irradiation under the same conditions without any visible phase transition. All the aforementioned fluids remained liquid for the period of at least one week when stored in darkness at room temperature. The fluid produced upon green-light irradiation of the hydrogel containing 20 g L^{-1} of **1** has been subsequently irradiated with violet light (410 nm LED, 9 mW cm^{-2}) for 60 min and incubated overnight (16 h) at room temperature in darkness. After that time, the sample turned into a transparent hydrogel again, with mechanical stability comparable to the non-irradiated sample (Fig. S5†). The internal fibrous structure of the hydrogels has been visualized using transmission electron microscopy (TEM) (Fig. S6†). We have also investigated gelation of **1** under a broader range of pH values in aqueous buffers at the constant concentration of 17 g L^{-1} of **1**. At the pH 10, the material did not dissolve up to the boiling point and no gelation was observed upon cooling. Samples buffered to the pH 4, pH 6, and pH 8 formed homogenous solutions above *c.a.* 60 °C, and upon short boiling formed homogenous hydrogels within 1 h of cooling at room temperature. The hydrogel formed at pH 4 was mechanically unstable and dissipated upon slight shaking or vial inversion. Hydrogels formed at pH 6 and pH 8 exhibited similar mechanical and thermal stability as the hydrogel prepared at the pH 7.4 from 17 g L^{-1} of **1**. (Fig. S3†).

Our next goal on the way to therapeutic relevance of our drug-releasing hydrogels was to minimize the passive cargo diffusion ("leaking") from non-irradiated gel samples, which previously varied between 5% and 30% of respective light-induced release rates. We noticed that the "leaking" is less pronounced for the cargo negatively charged under physiological conditions (*e.g.* DNA oligomers,[54] or carboxylic acids[55]). This was attributed to electrostatic interactions with the basic, positively charged lysine side chains, likely exposed on the fiber surface of the gel matrix. This interaction would, in turn, slow down the diffusion of acidic cargo through cavities of the gel matrix.

Here we decided to assume a different approach. Fast self-healing of our gels (<1 min, based on rheological determination of the storage modulus G' recovery upon 100% deformation, Fig. S5†) indicates its highly dynamic nature, where supramolecular interactions between monomeric units are quickly reconstituted upon deformation. We hypothesized that a cargo bearing the cyclic dipeptide motif connected to an aromatic residue would be promptly incorporated into the fibrous structure of the hydrogel (Fig. 2), instead of being absorbed in the cavities between fibers. As photoisomerization breaks the fibrous structures, the non-photochromic cargo would then be released from the supramolecular network upon hydrogel erosion.

Many clinically approved drugs contain the cyclic dipeptide motif (2,5-diketopiperazine, DKP) bound to aromatic residues. They show a broad spectrum of activities – to name only tadalafil (the active ingredient of "Cialis®" – a drug against erectile dysfunctions), retosiban (an oxytocin receptor inhibitor used for the treatment of premature birth), or aplaviroc (a CCR5 entry inhibitor developed for treatment of HIV infections).[57]

To test our hypothesis, we have selected a strong antiproliferative agent plinabulin (**2**) (Fig. 2), which is a promising anticancer drug candidate.[58] It acts as a low-nanomolar inhibitor of tubulin depolymerization, which hampers cytoskeleton dynamics. The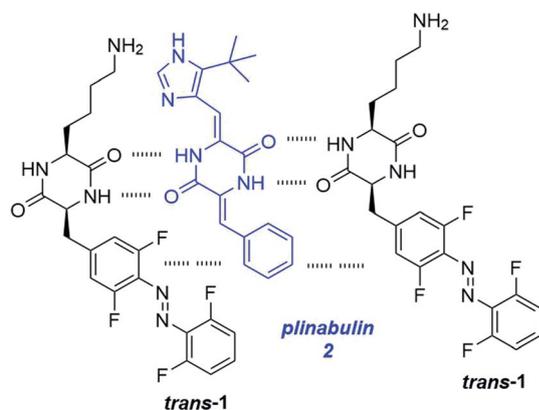 resulting mitotic arrest stops cell division and the cancer growth.[59] **2** shares structural similarities, in particular the cyclic dipeptide residue and an aromatic substituent, with the gelator **1**. We have synthesized **2** following a literature procedure (Scheme S2†).[60]

Afterwards we encapsulated **2** in the hydrogel composed of 17 g L^{-1} of **1** in PBS pH 7.4, and characterized its release upon dissipation of the gel resulting from green light irradiation. To our delight, the cargo could be recovered almost quantitatively in solution upon light-driven gel dissipation within 30 min, while "leaking" from identical gels incubated in darkness was negligible (below 1%, Fig. 3). For comparison, an antibiotic ciprofloxacin (with similar MW and a structure unrelated to the gelator **1**) encapsulated and released upon light-induced dissipation of the otherwise identical gel composition showed over 25% leaking in darkness within the same time period (Fig. S7†).

Due to limited solubility of plinabulin (**2**) in water, stock solutions of **2** were prepared in DMSO and diluted 100-fold in aqueous solutions for the final formulations. We determined the aqueous solubility of **2** (PBS pH 7.4, 1% DMSO) in absence of the gelator **1** to be 7.5 ± 1.7 µmol L^{-1} (2.5 mg L^{-1}). Above this concentration, visible precipitation appeared within 60 minutes from diluting the DMSO stock solutions with PBS (for the original drug, the issue of low water solubility was addressed *e.g.* by covalent functionalization with hydrophilic PEG groups).

However, hydrogels (17 g L^{-1} of **1**) comprising the compound **2** at final concentrations ≤350 µmol L^{-1} (118 mg L^{-1}) (by adding respectively more concentrated DMSO stock solutions during the preparation process) were still transparent and without any precipitation upon prolonged time (>16 h). This additionally supports the hypothesis that **2** is being incorporated into the supramolecular structure of the hydrogel upon its formation. The dopant **2** still constitutes below 1% of the dry mass of the gelator **1** used in the respective composition,
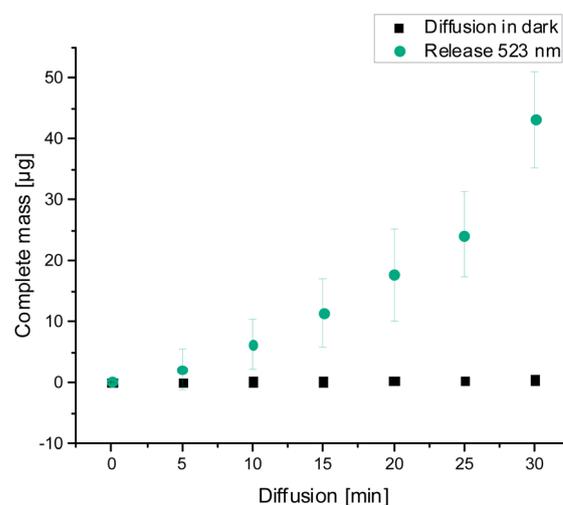

Fig. 2 Schematic representation of supramolecular interactions between the gelator **1** and a potent anticancer agent plinabulin (**2**). Hydrogen bonding and hydrophobic interactions of aromatic rings, most likely stabilize drug molecules inside of the fibrous network of the hydrogel and prevent its leaking in darkness.

Fig. 3 Light-induced release of encapsulated plinabulin **2** (56 µg) upon dissipation of the hydrogel (0.5 mL) containing 17 g L^{-1} of **1** caused by irradiation with green light (530 nm LED, 7 mW cm^{-2}) (green circles). Passive diffusion ("leaking") of **2** from the same hydrogel in darkness (black squares) is negligible. Suppression of the "leaking" is attributed to the supramolecular association of **2** and *trans*-**1** in fibres.

therefore no significant alterations of the gel physical properties (melting temperature, or mechanical strength) have been observed.

An important factor in potential therapeutic applications of the demonstrated drug-releasing material is the toxicity of the drug delivery vehicle to human cells. This was determined for our gelator **1** using cell viability assays (MTT assays). We have treated one human cancerous (HeLa) and one non-cancerous (NHDF – fibroblasts) cell line with increasing concentrations of the gelator **1** as pure *trans*-isomer (the thermally stable form that forms hydrogels in water), or as a mixture obtained upon irradiation of *trans*-**1** with green light until the respective photostationary state was achieved (this mixture corresponds to the dissipated hydrogel). In all but one combination (Fig. S9†) we observed no significant decrease in cell viability up to the concentrations of 1 mM of **1** (*c.a.* 0.45 g L^{-1}, slightly below the CGC values). Only in the case when cancerous HeLa cells were exposed to the pure *trans*-**1**, the cell viability strongly decreased above the concentration of 0.1 mM of the gelator **1**.

To further assess applicability of our composition for therapeutic purposes, we considered that the irradiation power required for the gel dissipation in our experiments (<10 mW cm^{-2}) is considerably lower than the safety limits determined for human tissues (200 mW cm^{-2}).[24] In contrast to photodynamic therapies (PDT) used clinically to treat malignant cancers,[61] tissues targeted with our gel composition would not need to be oxygenated. Furthermore, the clinically existing PDT infrastructure could be used for the release of **2** upon photodegradaton of our hydrogel.

In the future, the efficiency of our system will have to be confirmed *in vivo* (*e.g.* in model mice with tumor xenografts), before human therapeutic applications can be considered. Particularly suitable therapeutic targets for the currently presented composition seem to be retina cancers or squamous carcinoma (skin cancer), which appear in organs that can be efficiently penetrated with green light.

The composition demonstrated here could be further formulated as micro/nanogel (with eventual stabilization, *e.g.* by covering with biocompatible alginate), and injected into the bloodstream, or given upon inhalation. With the reported low-nanomolar antitumor potency of plinabulin **2** (IC$_{50}$ = 15 nM against human colon cancer HT-29 cells[60]), systemic introduction of such a microformulated hydrogel containing 0.35 mM of **2**, followed by its rapid and close-to-quantitative light-driven discharge in the selected area, should produce sufficiently high local drug concentration to successfully eradicate neighboring tumor cells. At the same time, the remaining drug will circulate in darkness in its inactive form (entrapped in the gel fibers), eventually metabolized and cleared from the organism over a prolonged period of time, thus minimizing the systemic toxicity and resulting in better therapeutic effect in comparison to neat plinabulin.

The remaining challenge is modification of the photochromic segment of our system to cause the gel dissipation upon irradiation with red or near-IR frequencies (within the so-called "therapeutic window" of light, 650–900 nm), capable of deep penetration (>1 cm) of soft human tissues. This would enable *e.g.* a general strategy for targeting of solid tumors inside of human organs without surgical intervention with established and efficient cytotoxic agents, yet with minimizing systemic side effects. Therefore, in the future we will examine the applicability of *ortho*-alkoxy and *ortho*-chlorinated azobenzenes, which were efficiently switched upon red light irradiation,[39,40] in our hydrogel systems.

Conclusions

In conclusion, we demonstrated that the gelator **1**, non-toxic for non-cancerous human cells below 1 mM concentrations, forms stable supramolecular hydrogels at and above concentrations of 15 g L^{-1} under physiological conditions and in the pH range 6–8. The gels can be reversibly dissipated to fluids with green light, and concomitantly release previously encapsulated cargo. Moreover, we identified a potent anticancer agent plinabulin **2** as an optimal therapeutic agent, which due to the structural similarity with **1** can be encapsulated and quickly released from the dissipating hydrogel upon irradiation, while its diffusion ("leaking") outside of the intact gel in darkness is negligible. The concentration of **2** in our supramolecular composition can be over 40-fold higher than its aqueous solutions, without disturbing the gel homogeneity. This additionally enhances delivery efficiency of **2** in therapeutic use.

Formulation of such compositions as injectable or inhalable micro/nanogels may enable systemic introduction into organisms. Subsequent cargo release with laser or LED green irradiation will produce a high local concentration of the cytotoxic agent. The local dose can be much higher than the concentration achieved upon simple drug injection, without causing severe side effects outside of the irradiation area, and thus enable faster and more efficient cancer eradication. Due to the penetration propensity of green light, eye and skin cancers remain the primary targets for this composition. In contrary to photodynamic therapies, the targeted tissues do not have to be oxygenated.

Extension of the described methodology to the red- or NIR-light-induced gel dissipation is also foreseen to enable targeting of solid human tumours on the organismal scale. The release of other drugs based on the cyclic dipeptide (DKP) motif will be also investigated.

Conflicts of interest

There are no conflicts to declare.

Acknowledgements

Notes and references

1 R. Narayanaswamy and P. V. Torchilin, Hydrogels and Their Applications in Targeted Drug Delivery, *Molecules*, 2019, **24**(3), 603.

2 J. Li and D. J. Mooney, Designing hydrogels for controlled drug delivery, *Nat. Rev. Mater.*, 2016, **1**, 16071.

3 M. H. Chen, *et al.*, Injectable Supramolecular Hydrogel/Microgel Composites for Therapeutic Delivery, *Macromol. Biosci.*, 2019, **19**, 1800248.

4 J. Y. C. Lim, Q. Lin, K. Xue and X. J. Loh, Recent advances in supramolecular hydrogels for biomedical applications, *Appl. Mater. Today*, 2019, **3**, 100021.

5 J. Shi, Y. Gao, Z. Yang and B. Xu, Exceptionally small supramolecular hydrogelators based on aromatic–aromatic interactions, *Beilstein J. Org. Chem.*, 2011, **7**, 167–172.

6 P. Chakraborty, *et al.*, Unusual Two-Step Assembly of a Minimalistic Dipeptide-Based Functional Hypergelator, *Adv. Mater.*, 2020, **32**, 1906043.

7 M. P. Conte, N. Singh, I. R. Sasselli, B. Escuder and R. V. Ulijn, Metastable hydrogels from aromatic dipeptides, *Chem. Commun.*, 2016, **52**, 13889–13892.

8 O. Bellotto, S. Kralj, R. De Zorzi, S. Geremia and S. Marchesan, Supramolecular hydrogels from unprotected dipeptides: a comparative study on stereoisomers and structural isomers, *Soft Matter*, 2020, **16**, 10151–10157.

9 P. Chakraborty, *et al.*, A Self-Healing, All-Organic, Conducting, Composite Peptide Hydrogel as Pressure Sensor and Electrogenic Cell Soft Substrate, *ACS Nano*, 2019, **13**, 163–175.

10 A. M. Garcia, *et al.*, Chirality Effects on Peptide Self-Assembly Unraveled from Molecules to Materials, *Chem.–Eur. J.*, 2018, **4**, 1862–1876.

11 K. J. Skilling, B. Kellam, M. Ashford, T. D. Bradshaw and M. Marlow, Developing a self-healing supramolecular nucleoside hydrogel, *Soft Matter*, 2016, **12**, 8950–8957.

12 A. J. Kleinsmann, N. M. Weckenmann and B. J. Nachtsheim, Phosphate-Triggered Self-Assembly of *N*-[(Uracil-5-yl)methyl]urea: A Minimalistic Urea-Derived Hydrogelator, *Chem.–Eur. J.*, 2014, **20**, 9753–9761.

13 V. Basavalingappa, *et al.*, Expanding the Functional Scope of the Fmoc-Diphenylalanine Hydrogelator by Introducing a Rigidifying and Chemically Active Urea Backbone Modification, *Adv. Sci.*, 2019, **6**, 1900218.

14 M. W. Tibbitt, J. E. Dahlman and R. Langer, Emerging Frontiers in Drug Delivery, *J. Am. Chem. Soc.*, 2016, **138**, 704–717.

15 A. N. Shy, B. J. Kim and B. Xu, Enzymatic Noncovalent Synthesis of Supramolecular Soft Matter for Biomedical Applications, *Matter*, 2019, **1**, 1127–1147.

16 J. Hoque, N. Sangaj and S. Varghese, Stimuli-Responsive Supramolecular Hydrogels and Their Applications in Regenerative Medicine, *Macromol. Biosci.*, 2019, **19**, 1800259.

17 M. Vázquez-González and I. Willner, Stimuli-Responsive Biomolecule-Based Hydrogels and Their Applications, *Angew. Chem., Int. Ed.*, 2020, **59**, 15342–15377.

18 L. Li, J. M. Scheiger and P. A. Levkin, Design and Applications of Photoresponsive Hydrogels, *Adv. Mater.*, 2019, **31**, 1807333.

19 E. Fuentes, *et al.*, An Azobenzene-Based Single-Component Supramolecular Polymer Responsive to Multiple Stimuli in Water, *J. Am. Chem. Soc.*, 2020, **142**, 10069–10078.

20 X. Li, Y. Gao, Y. Kuang and B. Xu, Enzymatic formation of a photoresponsive supramolecular hydrogel, *Chem. Commun.*, 2010, **46**, 5364–5366.

21 S. J. Wezenberg, C. M. Croisetu, M. C. A. Stuart and B. L. Feringa, Reversible gel–sol photoswitching with an overcrowded alkene-based bis-urea supergelator, *Chem. Sci.*, 2016, **7**, 4341–4346.

22 M. Akazawa, *et al.*, Photoresponsive dithienylethene-urea-based organogels with "reversed" behavior, *Org. Biomol. Chem.*, 2008, **6**, 1544–1547.

23 S. van der Laan, B. L. Feringa, R. M. Kellogg and J. van Esch, Remarkable Polymorphism in Gels of New Azobenzene Bis-urea Gelators, *Langmuir*, 2002, **18**, 7136–7140.

24 D. Wang, M. Wagner, H.-J. Butt and S. Wu, Supramolecular hydrogels constructed by red-light-responsive host–guest interactions for photo-controlled protein release in deep tissue, *Soft Matter*, 2015, **11**, 7656–7662.

25 H. Yan, *et al.*, Wholly Visible-Light-Responsive Host–Guest Supramolecular Gels Based on Methoxy Azobenzene and β-Cyclodextrin Dimers, *Langmuir*, 2020, **36**, 7408–7417.

26 B. P. Nowak and B. J. Ravoo, Photoresponsive hybrid hydrogel with a dual network of agarose and a self-assembling peptide, *Soft Matter*, 2020, **16**, 7299–7304.

27 Z. L. Pianowski, Recent Implementations of Molecular Photoswitches into Smart Materials and Biological Systems, *Chem.–Eur. J.*, 2019, **25**, 5128–5144.

28 L. Heinke, *et al.*, Photoswitching in Two-Component Surface-Mounted Metal–Organic Frameworks: Optically Triggered Release from a Molecular Container, *ACS Nano*, 2014, **8**, 1463–1467.

29 R. Klajn, Spiropyran-based dynamic materials, *Chem. Soc. Rev.*, 2014, **43**, 148–184.

30 S. Wiedbrauk, T. Bartelmann, S. Thumser, P. Mayer and H. Dube, Simultaneous complementary photoswitching of hemithioindigo tweezers for dynamic guest relocation, *Nat. Commun.*, 2018, **9**, 1456.

31 K. Kumar, *et al.*, A chaotic self-oscillating sunlight-driven polymer actuator, *Nat. Commun.*, 2016, **7**, 11975.

32 P. K. Kundu, *et al.*, Light-controlled self-assembly of non-photoresponsive nanoparticles, *Nat. Chem.*, 2015, **7**, 646.

33 Z. Wang, *et al.*, Tunable molecular separation by nanoporous membranes, *Nat. Commun.*, 2016, **7**, 13872.

34 A. A. Beharry, O. Sadovski and G. A. Woolley, Azobenzene Photoswitching without Ultraviolet Light, *J. Am. Chem. Soc.*, 2011, **133**, 19684–19687.

35 D. Bléger, J. Schwarz, A. M. Brouwer and S. Hecht, *o*-Fluoroazobenzenes as Readily Synthesized Photoswitches Offering Nearly Quantitative Two-Way Isomerization with Visible Light, *J. Am. Chem. Soc.*, 2012, **134**, 20597–20600.

36 M. Hammerich, *et al.*, Heterodiazocines: Synthesis and Photochromic Properties, Trans to Cis Switching within the Bio-optical Window, *J. Am. Chem. Soc.*, 2016, **138**, 13111–13114.

37 R. Siewertsen, *et al.*, Highly Efficient Reversible Z–E Photoisomerization of a Bridged Azobenzene with Visible Light through Resolved S1(nπ*) Absorption Bands, *J. Am. Chem. Soc.*, 2009, **131**, 15594–15595.

38 Y. Yang, R. P. Hughes and I. Aprahamian, Near-Infrared Light Activated Azo-BF2 Switches, *J. Am. Chem. Soc.*, 2014, **136**, 13190–13193.

39 M. Dong, *et al.*, Near-Infrared Photoswitching of Azobenzenes under Physiological Conditions, *J. Am. Chem. Soc.*, 2017, **139**, 13483–13486.

40 M. Dong, A. Babalhavaeji, S. Samanta, A. A. Beharry and G. A. Woolley, Red-Shifting Azobenzene Photoswitches for *in Vivo* Use, *Acc. Chem. Res.*, 2015, **48**, 2662–2670.

41 D. Bléger and S. Hecht, Visible-Light-Activated Molecular Switches, *Angew. Chem., Int. Ed.*, 2015, **54**, 11338–11349.

42 C. Knie, *et al.*, *ortho*-Fluoroazobenzenes: Visible Light Switches with Very Long-Lived Z Isomers, *Chem.–Eur. J.*, 2014, **20**, 16492–16501.

43 M. Kai, *et al.*, Switching Thin Films of Azobenzene-Containing Metal–Organic Frameworks with Visible Light, *Chem.–Eur. J.*, 2017, **23**, 5434–5438.

44 C. Sonia, *et al.*, Structural Effects in Visible-Light-Responsive Metal–Organic Frameworks Incorporating *ortho*-Fluoroazobenzenes, *Chem.–Eur. J.*, 2016, **22**, 746–752.

45 D. Samanta, *et al.*, Reversible photoswitching of encapsulated azobenzenes in water, *Proc. Natl. Acad. Sci. U. S. A.*, 2018, **115**, 9379–9384.

46 M. Wegener, M. J. Hansen, A. J. M. Driessen, W. Szymanski and B. L. Feringa, Photocontrol of Antibacterial Activity: Shifting from UV to Red Light Activation, *J. Am. Chem. Soc.*, 2017, **139**, 17979–17986.

47 L. Zhang, G. Linden and O. Vázquez, In search of visible-light photoresponsive peptide nucleic acids (PNAs) for reversible control of DNA hybridization, *Beilstein J. Org. Chem.*, 2019, **15**, 2500–2508.

48 B. Heinrich, K. Bouazoune, M. Wojcik, U. Bakowsky and O. Vazquez, *ortho*-Fluoroazobenzene Derivatives as DNA Intercalators for Photocontrol of DNA and Nucleosome Binding by Visible Light, *Org. Biomol. Chem.*, 2019, **17**, 1827–1833.

49 V. N. Georgiev, *et al.*, Area Increase and Budding in Giant Vesicles Triggered by Light: Behind the Scene, *Adv. Sci.*, 2018, **5**, 1800432.

50 J. Luo, S. Samanta, M. Convertino, N. V. Dokholyan and A. Deiters, Reversible and Tunable Photoswitching of Protein Function through Genetic Encoding of Azobenzene Amino Acids in Mammalian Cells, *ChemBioChem*, 2018, **19**, 2178–2185.

51 A. J. Kleinsmann and B. J. Nachtsheim, Phenylalanine-containing cyclic dipeptides – the lowest molecular weight hydrogelators based on unmodified proteinogenic amino acids, *Chem. Commun.*, 2013, **49**, 7818–7820.

52 A. J. Kleinsmann and B. J. Nachtsheim, A minimalistic hydrolase based on co-assembled cyclic dipeptides, *Org. Biomol. Chem.*, 2020, **18**, 102–107.

53 C. G. Pappas, *et al.*, Spontaneous Aminolytic Cyclization and Self-Assembly of Dipeptide Methyl Esters in Water, *ChemSystemsChem*, 2020, **2**, e2000013.

54 Z. L. Pianowski, J. Karcher and K. Schneider, Photoresponsive self-healing supramolecular hydrogels for light-induced release of DNA and doxorubicin, *Chem. Commun.*, 2016, **52**, 3143–3146.

55 J. Karcher and Z. L. Pianowski, Photocontrol of Drug Release from Supramolecular Hydrogels with Green Light, *Chem.–Eur. J.*, 2018, **24**, 11605–11610.

56 A. V. Razgulin and S. Mecozzi, Binding Properties of Aromatic Carbon-Bound Fluorine, *J. Med. Chem.*, 2006, **49**, 7902–7906.

57 A. D. Borthwick, 2,5-Diketopiperazines: Synthesis, Reactions, Medicinal Chemistry, and Bioactive Natural Products, *Chem. Rev.*, 2012, **112**, 3641–3716.

58 Z. Tian, *et al.*, Biological activity and interaction mechanism of the diketopiperazine derivatives as tubulin polymerization inhibitors, *RSC Adv.*, 2018, **8**, 1055–1064.

59 Z. Fu, *et al.*, Design, synthesis and biological evaluation of anti-pancreatic cancer activity of plinabulin derivatives based on the co-crystal structure, *Bioorg. Med. Chem.*, 2018, **26**, 2061–2072.

60 Y. Yamazaki, *et al.*, Synthesis and Structure–Activity Relationship Study of Antimicrotubule Agents Phenylahistin Derivatives with a Didehydropiperazine-2,5-dione Structure, *J. Med. Chem.*, 2012, **55**, 1056–1071.

61 J. Chen, *et al.*, New Technology for Deep Light Distribution in Tissue for Phototherapy, *Cancer J.*, 2002, **8**, 154–163.